Issues and characterization of fiber Bragg grating based temperature sensors in the presence of thermal gradients

Issues and Characterization of Fiber Bragg Grating Based Temperature Sensors in the Presence of Thermal Gradients

Riccardo Gassino, Jennifer Pogliano, Guido Perrone, Alberto Vallan

Department of Electronics and Telecommunications
Politecnico di Torino
Corso Duca degli Abruzzi, 24
Torino, 10129, Italy

Abstract

This paper reviews the main issues arising from the use of fiber Bragg gratings as temperature sensors in the presence of significant thermal gradients. These conditions occur for example during laser thermal ablation of tumors. In particular, the paper focuses on the identification of the grating position along the fiber, which represents one of the main uncertainty contributions. A novel experimental setup for the grating center localization is proposed and the corresponding characterization procedure has been devised. The setup is built in such a way as to generate reproducible linear temperature distributions. Tests carried out using a sensor prototype have shown that the grating position can be found with a standard uncertainty of 0.3 mm.

Keywords: quasi-distributed temperature measurement, fiber optic sensors, FBG, tumor laser ablation monitoring

1. Introduction

Fiber Bragg Gratings (FBG) inscribed in silica glass fibers are widely employed as temperature sensors both in industrial and biomedical applications because they combine the advantages typical of fiber optic sensors, with robust, technologically mature, and quite easy to use interrogation systems. In particular, FBGs are the elective temperature sensor in laser-based processes since in these cases common metallic sensors (e.g., thermocouples or thermistors) cannot be used as they partially absorb the laser light and thus perturb the temperature distribution. However, since commercially available FBGs are usually a few centimeters long, they only provide reliable readings when the temperature distribution is uniform along their length. An example of an application that makes use of FBG-based temperature sensors because it involves laser radiation, but is very critical because of the large temperature gradients, is temperature monitoring during Laser Ablation (LA) of tumors. This cancer treatment, which is an alternative to surgical resection, employs laser radiation to locally increase the tumor mass temperature above cytotoxic levels, causing cell death [1]. For deep-laying organs, such as in the cases of

liver or pancreas tumors, fiber optic applicators are used to deliver the laser radiation into the target area. Despite these kind of probes have already been employed in the medical field (for example in the treatment of cardiac diseases [2] and in cancer therapy [3]), their diffusion is still limited; and one reason is the lack of suitable sensors for real-time monitoring of the tissue temperature during the medical procedure [4]. Indeed, the effectiveness of LA requires a suitable combination of temperature and exposition time, being the two quantities inversely related. Usually, ablation treatments last from 2 min to 10 min and require reaching temperatures in the 60 °C to 100 °C range [5]. In in-vivo applications, however, it is practically impossible to estimate a priori the treatment duration necessary to obtain the targeted temperature from the laser power because of the large tissue variability and the blood perfusion. A solution has been to bundle [6] or inscribe into the laser delivery probe [7] one or more FBGs to measure the actual temperature increase. On the other hand, the use of FBGs poses some critical issues from the metrological point of view. For instance, the calibration of FBG sensors is routinely performed with respect to reference temperature sensors using climatic chambers or other controlled environments [8],[9],[10] in which the temperature is maintained constant at predefined values. Unfortunately, this is far from the operative conditions in LA, where gradients as large as 10 °C/cm occur due to low thermal conductivity of the organs. Therefore, as common FBGs present a length that spans from a millimeter to a couple of centimeters, the presence of a non-uniform temperature distribution can introduce unacceptable errors. Moreover, bare FBGs, which are often used to minimize the invasive impact [11] and the thermal inertia, can be affected by influence quantities, such as the bending introduced by patient breathing.

This paper investigates the most relevant aspects related to the qualification of FBGs as temperature sensors in non-uniform conditions, targeting in particular LA of liver tumors. Sect. 2 briefly recalls the FBG working principle and then introduces the main uncertainty contributions. Particular attention is given to the knowledge of the sensor position, which has not been considered so far in literature, but has to be known in order to significantly reduce temperature measurement errors. The solution proposed in the paper takes advantage of an experimental setup described in Sect. 3, and able to generate reproducible temperature gradients. Finally, Sect. 4 presents the experimental characterization results obtained with the help of the previously mentioned setup, whereas Sect. 5 draws the conclusions.

2. FBG working principle and measurement related issues

Working principle

FBG are manufactured by inducing a periodical modulation of the core refractive index of a single mode optical fiber. This results in the reflection of a specific group of wavelengths that depends on the grating period and on the modal effective index. Since these two quantities are related to the temperature and to the axial strain applied to the grating, the spectrum of the reflected light presents a narrow peak having a central position λ_B that can be computed with the following linear model:

$$\Delta\lambda_B = k_\epsilon \cdot \epsilon + k_T \cdot \Delta T \qquad (1)$$

where the sensitivity coefficients relating the wavelength shift respectively to the strain and to the temperature are approximatively $k_\epsilon = 1\,\mathrm{pm}/\epsilon$ and k_T $10\,\mathrm{pm}/^\circ\mathrm{C}$ for gratings having λ_B around 1500 nm. It is evident that the FBG acts as a temperature sensor provided that the strain is known or is kept constant. The temperature evolution can then be retrieved by tracking the Bragg wavelength using different standard interrogation techniques, such as that based on a broad-band source (typically a superluminescent LED, SLED) and a spectrometer or on a tunable laser and a power meter.

The following sections focus on the most significant issues arising when using the FBGs as temperature sensors, especially in the presence of non-negligible thermal gradients.

Strain cross-sensitivity

The cross-sensitivity of FBGs to both strain and temperature, clearly evident in Eq. 1, raises a series of problems in the practical use of the sensor, for example during a LA procedure. In this case the optical fiber containing the grating is inserted into the patient percutaneously through a suitable needle and this may induce axial strain and bending, which are then read by the FBG as temperature variations. Moreover, even if a perfect insertion is performed, the motion due to the patient breathing introduces artifacts. This problem can be mitigated by designing a suitable embodiment that encapsulates the FBG and prevents unwanted strain or bending from affecting the fiber. For LA applications the FBG sensors can be either inscribed in standard telecom single mode fibers (10/125 µm) bundled with the laser delivery fiber or inscribed in the same laser delivery fiber [7]. In both scenarios, to reduce the sensitivity to bending,

Figure 1: A schematic representation of the fiber with the FBG, inserted in a glass capillary and fixed on one side with epoxy resin.

the fiber portion containing the FBG (usually positioned towards the probe end) can be encapsulated in a glass capillary (Fig. 1).

With this solution, the capillary withstands the external stresses, although it affects the thermal properties of the probe since both the thermal capacity and the sensor time constant increase. Extensive tests in view of application to LA were previously carried out both with bare FBGs and with FBGs protected by different types of glass capillaries [12]. The results had shown that, at least for the considered capillaries, the time constant remains below about 0.2 s, a value that can be considered negligible for the intended application. However, the capillary not only affects the sensor dynamic response, but it can also absorb part of the laser radiation and this modifies the temperature distribution in the surrounding medium. In applications like LA, where the temperature presents a large gradient due to the high thermal resistance of the tissue, the sensor thermal properties (i.e., its thermal resistance and capacity) can be significantly different from those of the surrounding material and thus the presence of the capillary may significantly affect the temperature measurement. Of course, the closer is the capillary to the delivery fiber, the more evident is the effect of the absorption; therefore particular attention should be paid to probes that combine the laser delivery and the sensing fiber inside the same capillary. This introduces a systematic error than is almost impossible to model if

the surrounding material properties are not well known. Again, LA represents a critical case since the tissue properties are subjected to a large variability, even within the same organ. A possible solution is to minimize the error by reducing the probe dimensions and by using materials having tissue-matching thermal properties. However, the actual error can only be assessed though an experimental approach. Therefore, to quantify this perturbation tests were carried out by placing the laser in front of the encapsulated sensor and recording the temperature increase in free space, which represents the worst case condition for the almost null thermal conductivity. The results showed a temperature increase up to 0.5 °C/W for capillaries with external diameter of 1 mm and even higher values for thicker capillaries.

FBG length

The linear relation between Bragg wavelength and temperature in Eq. 1 is found considering a constant temperature distribution along the grating. This does not represent a limitation in applications in which thermal gradients are small (for example in structural health monitoring), but introduces large errors when a significant thermal gradient is present along the grating axis, like in LA: as commercial sensors can be as long as 2 cm, the sensor surface is exposed to a temperature difference that can be as large as 20 °C. FBG response in the presence of non-uniform conditions was addressed in a theoretical way for strain measurements [13] and the results showed a dependency of the Bragg wavelength with the gradient shape. This means that the sensor cannot be used to successfully recover the temperature value if the thermal distribution is unknown. Nevertheless, if the temperature distribution is linear, it is possible to demonstrate that the Bragg wavelength is proportional to the grating average temperature through the same sensitivity constant found for a uniform temperature distribution (Eq. 1). Short FBGs can partially solve this issue; however, they are not off-the-shelf products and present a large spectral response that could prevent an accurate estimation of the Bragg wavelength.

FBG position

The accurate knowledge of the sensor position with respect to the region whose temperature is under measurement is of great importance when large gradients are present. For commercial FBGs this problem is particularly significant since their location along the fiber axis is provided with an error of the order of a few millimeters, and this may introduce unacceptable temperature errors even for moderate gradients.

The error due to the sensor position is experimentally addressed in the next sections of the paper. The proposed approach takes advantage of the grating sensitivity to the average temperature in the presence of linear gradients. Consequently, when the grating is exposed to a linear temperature distribution, it provides the value of the average temperature, corresponding to the temperature at the center of the grating. In this way it is thus possible to relate the grating measurement to the grating position.

3. Setup for linear temperature distributions

The impact of non uniform temperature distributions on the actual reading from FBG-based temperature sensors is experimentally evaluated with the help of a characterization setup able to generate

linear temperature distributions with programmable gradients. The setup makes use of a 40 mm × 10 mm × 2 mm rectangular aluminum bar, which is heated on one side by a resistor and cooled on the opposite side by a Peltier cell (Fig. 2). Balancing the power consumption of the resistor and of the Peltier cell, with this setup is possible to reach up to 100 °C at the hot side, with gradients up to 2 °C/mm in the direction reported in Fig. 2. This range of temperature perfectly fits the one of the considered application, where the aim is to measure temperature increase in the range of 45 °C to 100 °C. A groove along the bar axis allows the repeatable positioning of the FBG sensor under characterization. The bar was graduated with 1 mm equally spaced spaced marks and three type-T thermocouples were inserted in 0.5 mm holes having depth of 8 mm in order to measure the bar temperature. The holes were then filled with heat-conductive paste.

The aluminum bar presents a uniform cross-section and thus provides a linear thermal gradient when the cooler and the heater are operating in steady-state conditions [14]. The temperature T at position p along the bar can be therefore expressed with the following linear model:

$$T = g \cdot p + T_0 \tag{2}$$

where g is the temperature gradient and T_0 is the temperature at the hot end of the bar (left-hand side in Fig. 2).

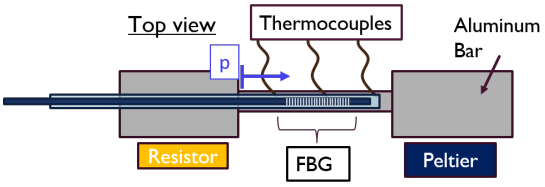

Figure 2: Schematic representation of the adopted setup for the generation of a linear temperature gradient. The FBG under characterization is positioned in the region between three thermocouples used as reference.

The parameters g and T_0 were computed using a best fitting algorithm that processes the thermocouple measurements T_i and their positions p_i as follows:

$$g = \frac{N\sum_{\mathrm{i}=1}^{\mathrm{N}} p_\mathrm{i}T_\mathrm{i} - \sum_{\mathrm{i}=1}^{\mathrm{N}} p_i \sum_{\mathrm{i}=1}^{\mathrm{N}} T_\mathrm{i}}{N\sum_{\mathrm{i}=1}^{\mathrm{N}} p_\mathrm{i}^2 - \left(\sum_{\mathrm{i}=1}^{\mathrm{N}} p_\mathrm{i}\right)^2} \tag{3}$$

$$T_0 = \frac{\sum_{\mathrm{i}=1}^{\mathrm{N}} T_i \sum_{\mathrm{i}=1}^{\mathrm{N}} p_\mathrm{i}^2 - \sum_{\mathrm{i}=1}^{\mathrm{N}} p_\mathrm{i} \sum_{\mathrm{i}=1}^{\mathrm{N}} (p_\mathrm{i}T_\mathrm{i})}{N\sum_{\mathrm{i}=1}^{\mathrm{N}} p_\mathrm{i}^2 - \left(\sum_{\mathrm{i}=1}^{\mathrm{N}} p_\mathrm{i}\right)^2} \tag{4}$$

where N is the number of thermocouples, hence the number of positions at which the temperature is measured.

The most significant uncertainty contributions are related to the thermocouples and to the bar non-uniformities, which affect the linearity of the distribution. As for the thermocouples contribution, the uncertainties were propagated using a Monte Carlo method. The thermocouples had been previously characterized in a climatic chamber with respect to a calibrated reference sensor, providing an uncertainty of $u_{\mathrm{T_i}} = 0.12\,°\mathrm{C}$. The thermocouple measurements are partially correlated, however a

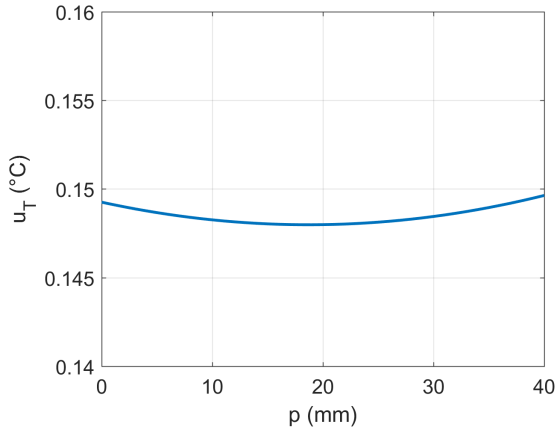

Figure 3: Plot of the standard uncertainty computed with the Monte Carlo method along the bar.

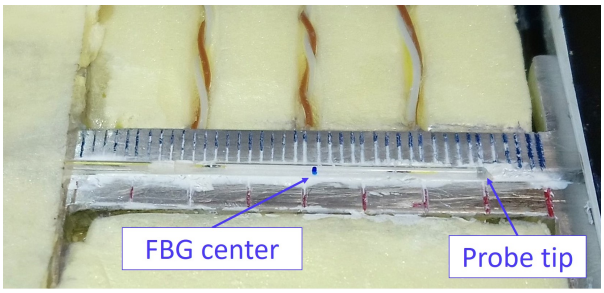

Figure 4: Picture of the setup showing the sensor probe placed in the bar groove with thermal paste. The blue mark on the glass capillary identifies the sensor central position.

full correlation was here considered in order to be conservative. The uncertainty $u_{\mathrm{p_i}}$ of the thermocouple position depends on the hole dimension and on the accuracy of the drilling tool. In our setup the former is negligible with respect to the latter; consequently, a rectangular distribution having the width of the hole diameter was assumed, thus $u_{\mathrm{p_i}} = 0.14\,\mathrm{mm}$.

As an example of uncertainty evaluation, the setup was programmed in order to provide a gradient of about $-2\,^{\circ}\mathrm{C/mm}$. The standard uncertainty of the temperature along the bar was numerically computed on the basis of the measured temperatures. The simulation results are shown in Fig. 3, where it is possible to see that the temperature standard uncertainty is almost constant with the position and it is about $0.15\,^{\circ}\mathrm{C}$.

The linearity of the temperature distribution δ_L was evaluated as the maximum difference between the temperature measured by the sensors and the temperature obtained with the linear model, yielding δ_L=0.5 °C. The sensors provide information on three points of the bar only; therefore an

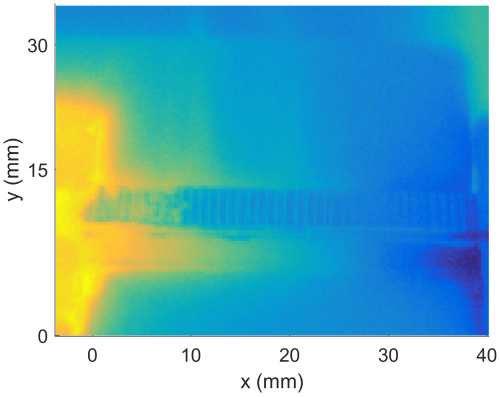

Figure 5: IR picture of the setup where the lower side of the bar has been made opaque in order to measure the temperature on the surface.

InfraRed (IR) camera (Fluke model Ti10) with spatial resolution of 0.5 mm was also employed. Fig. 5 shows an infrared image of the bar and Fig. 6 reports the temperature along the bar axis as well as the linear fitting. The camera noise (Fig. 7) provides an upper-bound to the estimation of the temperature linearity but it shows that the thermocouple measurements are representative of the bar non-uniformities.

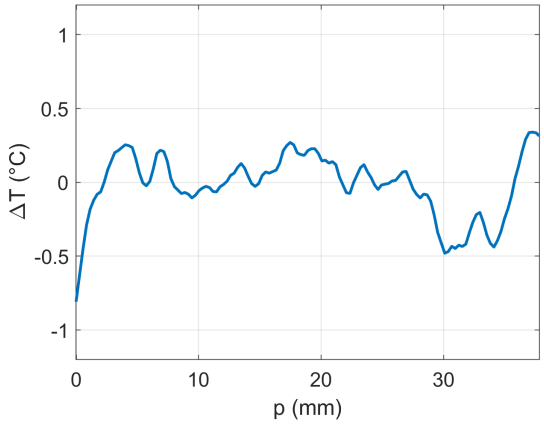

Figure 7: Camera noise obtained as the difference between the points taken from the IR camera and the linear best fit curve.

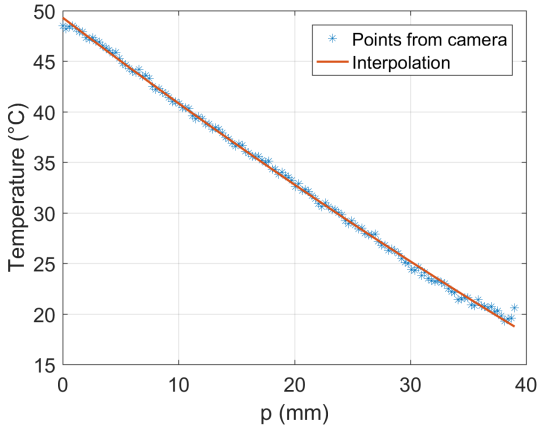

Figure 6: Linear interpolation of the points taken from the IR camera along a line in the opaque region where T_0 =49 °C and g=−0.8 °C/mm

The overall uncertainty (u_{Ttot}) of the bar temperature can be therefore obtained by combining the standard uncertainty of the bar (u_{T}) with the non-linearity, considered as uniformly distributed, thus obtaining $u_{Ttot} = \sqrt{u_T^2 + \delta_L^2/3} = 0.33\,^{\circ}\mathrm{C}$.

4. FBG Characterization

The setup was used to assess the behavior of a FBG sensor under non-uniform temperature distributions. First the uncertainty of a temperature sensor made by an FBG embedded in a glass capillary in uniform temperature conditions was evaluated using a climatic chamber. To this end a commercial 15 mm long FBG, with 90% reflectivity, 1550 nm central wavelength, and 0.3 nm Full-Width at Half Maximum (FWHM) was embedded in a 1 mm (external diameter) capillary, as shown in Fig. 1. The characterization showed that the FBG employed as temperature sensor has a standard uncertainty $u_{\mathrm{T_{FBG}}}$=0.4 °C, in the range of 0 °C to 100 °C, which is mainly due to the characterization procedure.

The sensor was then positioned on the bar in correspondence of the groove. Thermal-conductive paste was employed to improve the thermal transfer between the capillary and the bar. The capillary and the bar where then covered with an insulating sheet in order to minimize errors due to thermal convection.

The grating position inside the fiber was assessed with a thermal gradient of about −2 °C/mm. The grating temperature was measured from the Bragg wavelength, which is related to the grating position. Indeed, for a linear thermal distribution, the measured temperature is the value at the middle of the grating. The capillary was then moved along the bar until the measured temperature equaled the temperature at the middle of the bar. The obtained FBG position was marked.

The position uncertainty was then estimated on the basis of three main contributions: 1) the bar temperature uncertainty, 2) the FBG temperature uncertainty, and 3) the accuracy of the position determination on the bar. Working with a gradient of 2 °C/mm, contributions 1) and 2) correspond to a posi-

tion uncertainty of 0.16 mm and 0.2 mm, respectively, whereas contribution 3) is due to the accuracy of the marks on the bar and can be assumed to be ±0.25 mm, uniformly distributed. Considering the contributions uncorrelated, the overall uncertainty in the grating position is $u_{pFBG} = \sqrt{0.16^2 + 0.2^2 + (0.25/\sqrt{3})^2} = 0.3$ mm.

As a preliminary verification of the proposed characterization procedure, a reproducibility test was carried out with the same setup. The capillary was placed again on the bar at position $p = 20$ mm. The heater and cooler were then turned on and the temperatures measured with both thermocouples and the grating were recorded. Fig. 8 shows the temperature evolution of thermocouples T_1 and T_3, located at positions $p_1 = 10$ mm and $p_3 = 30$ mm, the expected temperature T_{p20} at $p_3 = 20$ mm, as obtained from Eq. 2, and the temperature T_{FBG} measured with the grating. It is possible to see that the grating temperature is close to T_{20} even during the thermal transient. When steady-state conditions are reached, the temperature difference is about 0.1 °C, which is in agreement with the expected uncertainty.

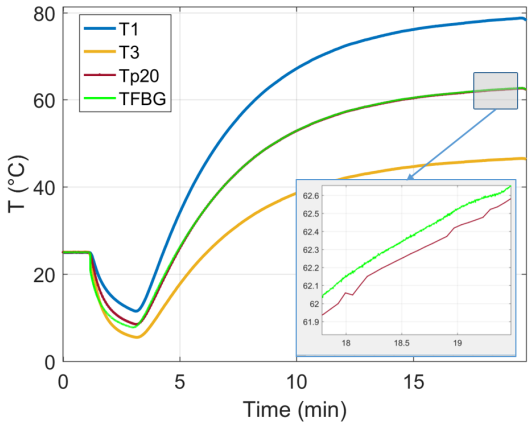

Figure 8: Evolution of the temperatures measured by thermocouples in p_{10}, p_{30} and their average (green), compared with the FBG measure (red).

5. Conclusions

The main issues related to the calibration of FBGs as temperature sensors in non-uniform conditions have been discussed in this paper, with particular reference to the case of tumor laser ablation, which represents a challenging application from the metrological point of view, given the typical large temperature gradients. The standard calibration procedure turned out to be useful in providing the sensor sensitivity, but in the presence of severe thermal gradients, as occurs during LA, the procedure is not able to properly asses the sensor accuracy.

Actually, the temperature distribution along the grating has an effect on the sensor response and it has been proven that in the case of a linear behavior the sensor provides the average temperature, that is, the temperature at the grating center. This position is rarely provided by the manufacturer with the required accuracy and it is thus responsible for a relevant uncertainty contribution, which is almost always not considered or underestimated. To this aim, a setup based on a metallic bar, which is able to generate highly reproducible and well-known linear temperature gradients, was built and employed to characterize temperature sensors made by standard FBGs embodied in strain-protective glass capillaries. The traceability of the generated thermal gradient is entrusted to electronic sensors and to a careful thermal design. Results showed that with this setup and with an FBG having length of 15 mm and able to measure temperatures in the range of 0 °C to 100 °C with a standard uncertainty of

0.4 °C, it is possible to locate the FBG position with a standard uncertainty of 0.3 mm. The effect of this contribution to the overall temperature uncertainty depends on the actual temperature gradients. In case of the sensor located close to the ablation area where gradients as large as 2 °C/mm are present, an uncertainty contribution of 0.6 °C must be taken into account.

References

[1] T. J. Vogl, K. Eichler, R. Straub, K. Engelmann, S. Zangos, D. Woitaschek, M. Bttger, M. G. Mack, Laser-induced thermotherapy of malignant liver tumors: general principals, equipment(s), procedure(s) side effects, complications and results, European Journal of Ultrasound 13 (2) (2001) 117 – 127. doi:https://doi.org/10.1016/S0929-8266(01)00125-2.

[2] D. Keane, New catheter ablation techniques for the treatment of cardiac arrhythmias, Cardiac Electrophysiology Review 6 (4) (2002) 341–348. doi:10.1023/A:1021115804352.

[3] P. Saccomandi, G. Quero, R. Gassino, A. Lapergola, L. Guerriero, M. Diana, A. Vallan, G. Perrone, E. Schena, G. Costamagna, J. Marescaux, F. M. D. Matteo, Laser ablation of the biliary tree: in vivo proof of concept as potential treatment of unresectable cholangiocarcinoma, International Journal of Hyperthermia 0 (0) (2018) 1–9, pMID: 29322853. doi:10.1080/02656736.2018.1427287.

[4] E. Schena, D. Tosi, P. Saccomandi, E. Lewis, T. Kim, Fiber optic sensors for temperature monitoring during thermal treatments: An overview, Sensors 16 (7). doi:10.3390/s16071144.

[5] R. W. Habash, R. Bansal, D. Krewski, H. T. Alhafid, Thermal therapy, part iii: ablation techniques, Critical Reviews in Biomedical Engineering 35 (1-2).

[6] Y. Liu, R. Gassino, A. Braglia, A. Vallan, G. Perrone, Fibre probe for tumour laser thermotherapy with integrated temperature measuring capabilities, Electronics Letters 52 (2016) 798–800(2).

[7] R. Gassino, Y. Liu, M. Konstantaki, A. Vallan, S. Pissadakis, G. Perrone, A fiber optic probe for tumor laser ablation with integrated temperature measurement capability, J. Lightwave Technol. 35 (16) (2017) 3447–3454.

[8] G. Yang, C. Leito, Y. Li, J. Pinto, X. Jiang, Real-time temperature measurement with fiber bragg sensors in lithium batteries for safety usage, Measurement 46 (9) (2013) 3166 – 3172.

[9] D. Wada, H. Murayama, H. Igawa, K. Kageyama, K. Uzawa, K. Omichi, Simultaneous distributed measurement of strain and temperature by polarization maintaining fiber bragg grating based on optical frequency domain reflectometry, Smart Materials and Structures 20 (8) (2011) 085028.

[10] J. Lauzon, S. Thibault, J. Martin, F. Ouellette, Implementation and characterization of fiber bragg gratings linearly chirped by a temperature gradient, Opt. Lett. 19 (23) (1994) 2027–2029. doi:10.1364/OL.19.002027.

[11] R. mei Liu, D. kai Liang, A. Asundi, Small diameter fiber bragg gratings and applications, Measurement 46 (9) (2013) 3440 – 3448.

[12] W. Chen, R. Gassino, Y. Liu, A. Carullo, G. Perrone, A. Vallan, D. Tosi, Performance assessment of fbg temperature sensors for laser ablation of tumors, in: 2015 IEEE International Symposium on Medical Measurements and Applications (MeMeA) Proceedings, 2015, pp. 324–328. doi:10.1109/MeMeA.2015.7145221.

[13] H. yin Ling, K. tak Lau, L. Cheng, K. wing Chow, Embedded fibre bragg grating sensors for non-uniform strain sensing in composite structures, Measurement Science and Technology 16 (12) (2005) 2415.

[14] R. Gassino, A. Vallan, G. Perrone, M. Konstantaki, S. Pissadakis, Characterization of fiber optic distributed temperature sensors for tissue laser ablation, in: 2017 IEEE International Instrumentation and Measurement Technology Conference (I2MTC), 2017, pp. 1–5. doi:10.1109/I2MTC.2017.7969862.